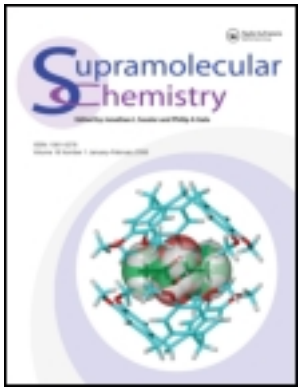

Supramolecular Chemistry
Publication details, including instructions for authors and subscription information:
http://www.tandfonline.com/loi/gsch20

Sensitive fluorescent vesicles based on the supramolecular inclusion of β-cyclodextrins with *N*-alkylamino-l-anthraquinone

Tao Sun [a], Huacheng Zhang [a], Hui Yan [a], Jianye Li [a], Guanghui Cheng [b], Aiyou Hao [a], Hongwei Qiao [c] & Feifei Xin [a]

[a] Key Laboratory of Colloid and Interface Chemistry, Ministry of Education, School of Chemistry and Chemical Engineering, Shandong University, Jinan, 250100, P.R. China

[b] Department of Medical Genetics and Key Laboratory for Experimental Teratology, Ministry of Education, Shandong University, Jinan, 250012, P.R. China

[c] Shandong Shengquan Chemical Co., Ltd, Jinan, 250204, P.R. China

Available online: 15 Apr 2011

To cite this article: Tao Sun, Huacheng Zhang, Hui Yan, Jianye Li, Guanghui Cheng, Aiyou Hao, Hongwei Qiao & Feifei Xin (2011): Sensitive fluorescent vesicles based on the supramolecular inclusion of β-cyclodextrins with *N*-alkylamino-l-anthraquinone, Supramolecular Chemistry, 23:05, 351-364

To link to this article: http://dx.doi.org/10.1080/10610278.2010.514614

Supramolecular Chemistry
Vol. 23, No. 5, May 2011, 351–364

Taylor & Francis
Taylor & Francis Group

Sensitive fluorescent vesicles based on the supramolecular inclusion of β-cyclodextrins with *N*-alkylamino-L-anthraquinone

Tao Sun[a†], Huacheng Zhang[a†], Hui Yan[a], Jianye Li[a], Guanghui Cheng[b], Aiyou Hao[a]*, Hongwei Qiao[c] and Feifei Xin[a]

[a]*Key Laboratory of Colloid and Interface Chemistry, Ministry of Education, School of Chemistry and Chemical Engineering, Shandong University, Jinan 250100, P.R. China;* [b]*Department of Medical Genetics and Key Laboratory for Experimental Teratology, Ministry of Education, Shandong University, Jinan 250012, P.R. China;* [c]*Shandong Shengquan Chemical Co., Ltd, Jinan 250204, P.R. China*

(*Received 25 April 2010; final version received 28 July 2010*)

Self-assembly fluorescent vesicles were designed and prepared based on the supramolecular interaction of cyclodextrins and *N*-alkylamino-L-anthraquinone (*n*-AQ). As the guest molecules, *n*-AQs with alkyl lengths ranging from C_0 to C_{18} were synthesised by the direct reaction of alkylamine with L-nitroanthraquinone in *N*,*N*-dimethylformamide. Transmission electron microscopy (TEM), scanning electron microscopy, dynamic light scattering and epi fluorescence microscopy were employed to study the vesicle system in detail. The formation mechanism of the vesicles was suggested based on the results of TEM observation, UV spectrum, fluorescence spectrum, ^{1}H NMR and simulation in the software Materials 4.3. The fluorescent vesicles show sensitive and multi-responsive properties to external stimuli. Based on these properties, we tried to use the vesicle as a new kind of fluorescence staining material for living cells. The vesicles can effectively stain the human breast cancer cells (MCF-7) and mice mononuclear macrophages (REW-264.7). This paper provides a better understanding in the design and preparation of drug delivery, biomaterials and intelligent materials.

Keywords: vesicles; fluorescence; cyclodextrins; sensitive; supramolecular amphiphile

1. Introduction

Cyclodextrins (CDs) are a series of α-1,4-linked cyclic oligosaccharides composed of 6, 7 or 8 D-(+)-glucose repeat units corresponding to α-, β- and γ-CDs, respectively (*1*). Self-assembly vesicles made from CDs are utilised extensively for their combined properties of liposomes and macro-cyclic host molecules (*2–4*), which creates a great potential for the development of encapsulating and solubilisation of drugs, or the recognisation and combination of the specific types of guest molecules (*5–8*).

It has been found that CDs can complex various guest molecules (*9–11*), which may be applied to building novel 'supramolecular amphiphiles' (*12*, *13*) (Figure 1). The self-assembly of 'supramolecular amphiphiles' into vesicles can be effective and simple, but is complicated by modified CDs (*14*). It can be inferred that the inclusion phenomenon plays the key role in combining the hydrophobic tail and the hydrophilic head together. It is known that the supramolecular inclusion is affected by some stimuli (*1*, *5–8*), which also means that the vesicles based on the supramolecular amphiphiles are multi-responsive and may therefore be applied in the targeted release of some special molecules.

Aggregates assembled by supramolecular amphiphiles are more promising in developing responsive drug-carrier systems with the ability to target-release (*12–15*). Considerable research has been done to study the effect of hydrophobic tail lengths, the composition of the amphiphilic surfactant or the change of the solvent on the formation of aggregates in the general amphiphilic surfactant solution (*16–20*). However, there are still few reports on the topic of 'supramolecular amphiphiles'. In this paper, we describe in detail the designation, preparation and application of a family of vesicles based on the supramolecular interactions of *n*-AQ and β-CD, or 2-*O*-hydroxypropyl-β-cyclodextrin (HP-β-CD). The vesicles were visualised with transmission electron microscopy (TEM), scanning electron microscopy (SEM), dynamic light scattering (DLS), epi fluorescence microscopy (EFM) and the mechanism was suggested based on the experimental results of UV, fluorescence spectrum, ^{1}H NMR and simulation in the software Materials 4.3. We discuss the effects of hydrophobic tail lengths and the change of the solvent composition on the formation of vesicles.

The vesicles showed sensitive and multi-responsive properties to external stimuli. Based on these properties, we managed to use the vesicle as a new kind of fluorescence

*Corresponding author. Email: haoay@sdu.edu.cn
† These authors contributed equally to this work.

ISSN 1061-0278 print/ISSN 1029-0478 online

DOI: 10.1080/10610278.2010.514614
http://www.informaworld.com

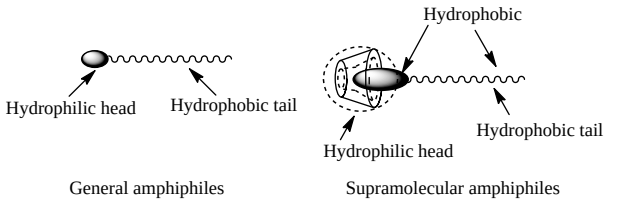

Figure 1. Comparison between general amphiphiles and supramolecular amphiphiles.

staining material for living cells; however, there are still more theoretical than practical applications of vesicles. It was found that the chosen cells were stained evenly and effectively. We believe that this study may provide a promising new method to design artificial supramolecular systems to be used in biomaterials. The vesicle system could also provide new references in intelligent materials, medicine and pharmacy, and may turn over a new leaf for the practical application of vesicles.

2. Experimental

2.1 Materials

L-Nitroanthraquinone, *N*-methylamino-L-AQ (L-AQ) and L-aminoanthraquinone (*n*-AQ) were gifts from Shandong Aokete Chemical Reagent Co. Ltd, China. β-CD was purchased from Guangdong Yunan Chemical Reagent Co. Ltd, China and recrystallised twice from distilled water and dried by vacuum for 12 h. HP-β-CD, with an $n = 4.8$ substituting degree, was purchased from Zibo Xinda Chemical Reagent Co. Ltd, China. *N*,*N*-Dimethylformamide (DMF) was first dried by $MgSO_4$ for 24 h and then distilled by vacuum. All other reagents were purchased from Country Medicine Reagent Co. Ltd, China. All these other organic reagents were analytically pure and used as received. Ampicillin, piroxicam, simvastatin and amoxicillin were supplied by Jien Medicament Research Company, China. Thin layer chromatography (TLC) analysis was performed on glass plates precoated with silica gel F_{254}, which were obtained from Qingdao Haiyang Chemical, China. The developer used was ethyl acetate–petroleum ether (1:5, by volume).

MCF-7, REW-264.7 and HeLa cells were cultured in the DMEM medium, at 36.5 ± 0.5°C, 5% CO_2, pH = 7.0–7.4 and a permeate pressure = 0.26–0.32 mol/l. Cell suspensions, which meet counting requirements, were filled in corresponding flasks with a proper culture medium, placed in the incubator for 3 h, and then cultured continuously after replacing the medium. Phosphate buffered saline (PBS) was prepared by adding 8.5 g NaCl, 2.85 g $Na_2HPO_4 \cdot 12H_2O$, 0.2 g KCl and 0.27 g KH_2PO_4 into 1000 ml distilled water and then sonicated for 20 min at 300 K.

2.2 Measurements and methods

^1H and ^{13}C NMR spectra were carried out on API Bruker Avance 400 M NMR at room temperature (r.t.) with CD_3COCD_3 as the solution and TMS as the reference. The experiment of chemical shifts of H between 18-AQ/β-CD and β-CD was carried out in a solution of 10^{-5} mol/l in D_2O and CD_3OD (1:1, by volume). IR spectra were obtained on an Avatar 370 FT-IR spectrometer.

All samples for TEM were prepared by the phosphotungstic acid staining technique using a JEM-100CX electron microscope. SEM images were obtained with the Hitachi S-4800 scanning electron microscope by coating the vesicular solution to the base plate and then dried and sputter-coated with gold.

DLS measurements were carried out with the Wyatt QELS Technology DAWN HELEOS instrument poised at r.t. by using a 12-angle replaced detector in a scintillation vial and a 50 mW solid-state laser ($\lambda = 658.0$ nm). All solutions used in DLS were filtered through a 0.45 μm filter before detection.

UV/vis spectra were recorded at r.t. with a TU-1800pc UV/vis spectrophotometer. The fluorescence spectrum was taken using a Hitachi F-4500 spectrophotometer (Japan) operated at an excitation wavelength of 488 nm and a slit width of 10 nm. QDs at a concentration of 1.0×10^{-9} M were measured both in PBS (pH = 7.4) solution and borate buffer solution (pH = 8.3). All measurements were performed at r.t.

EFM imaging was performed with an Olympus IX81 fluorescence microscope (Tokyo, Japan) equipped with a high-numerical-aperture 60 × (1.45 NA) and 100 × (1.40 NA) oil-immersion objective lens, a mercury lamp source, a mirror unit consisting of a 330–385 nm excitation filter (BP330-385), a 455 nm dichromatic mirror (DM 455), an emission filter (IF510-550) and a 16-bit thermoelectrically cooled EMCCD (Cascade 512B; Tucson, AZ, USA). Imaging acquisition and data analysis were performed using MetaMorph software (Universal Imaging, Downingtown, PA, USA).

Fluorescence microscopy was performed with an Olympus IX71 fluorescence microscope (Tokyo, Japan) equipped with a high-numerical-aperture 100 × (1.40 NA) oil-immersion objective lens, a mercury lamp source, ultraviolet light emission and fluorescence detection mode.

The sonication was performed on KQ116 ultrasonic cleaners, Kunshan ultrasonic apparatus Co. Ltd, China.

2.3 Synthesis and characterisation of n-AQ

Alkylamine directly reacted with L-nitroanthraquinone in DMF without a catalyst, to prepare nine anthraquinone derivates (*n*-AQs): *N*-isopropylamino-L-anthraquinone (3^i-AQ), *N*-*n*-butylamino-L-anthraquinone (4-AQ), *N*-cyclohexylamino-L-anthraquinone (6^c-AQ), *N*-*n*-hexylamino-L-anthraquinone (6-AQ), *N*-*n*-decylamino-L-anthraquinone

Table 1. Synthesis of *n*-AQs.

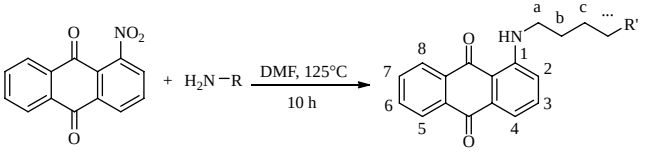

Entry	R-NH_2	Product
3^i-AQ	H_2N—	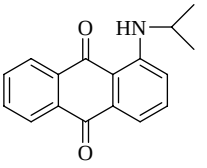
4-AQ	$NH_2(CH_2)_3CH_3$	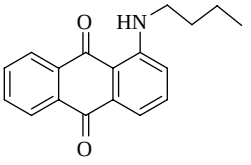
6^c-AQ	H_2N—	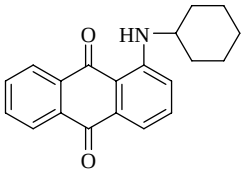
6-AQ	$NH_2(CH_2)_5CH_3$	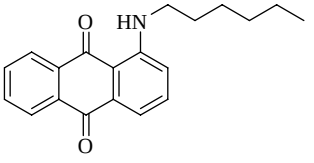
10-AQ	$NH_2(CH_2)_9CH_3$	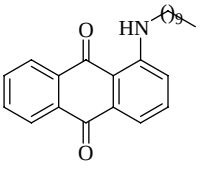
12-AQ	$NH_2(CH_2)_{11}CH_3$	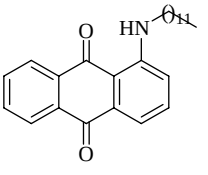
14-AQ	$NH_2(CH_2)_{13}CH_3$	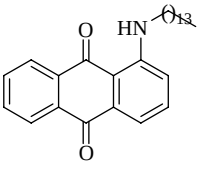
16-AQ	$NH_2(CH_2)_{15}CH_3$	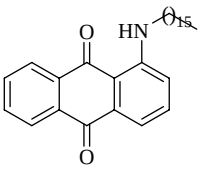
18-AQ	$NH_2(CH_2)_{17}CH_3$	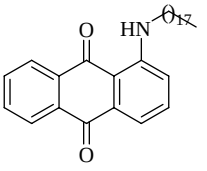

(10-AQ), *N*-*n*-dodecylamino-L-anthraquinone (12-AQ), *N*-*n*-tetradecyl-L-anthraquinone (14-AQ), *N*-hexadecylamino-L-anthraquinone (16-AQ) and *N*-octadecylamino-L-anthraquinone (18-AQ) (Table 1). This method is more convenient than the previous method (*21*). DMF was chosen for its excellent solubility.

L-Nitroanthraquinone (2.01 g, 8 mmol) was allowed to react with alkylamine (16 mmol) in DMF (8 ml) at 125°C, refluxing for 10 h. The reaction was monitored by TLC. The reaction mixture was then cooled and poured into water, and filtered under reduced pressure. The crude product was washed with water, and further purified by silica gel column chromatography with a mixture eluent of ethyl acetate with petroleum ether (1:20, by volume).

2.4 Characterisation of n-AQ

2.4.1 Data of 3^i-AQ

Red powder; mp = 195–197°C; Yield, 94%; $R_f = 0.65$; ^{1}H NMR (TMS, δ ppm): 8.32–8.30 (q, 1H, H-6^{AQ}), 8.22–8.20 (q, 1H, H-7^{AQ}), 7.90–7.84 (m, 2H, H-5^{AQ}, H-8^{AQ}), 7.68–7.64 (q, 1H, H-3^{AQ}), 7.54–7.52 (q, 1H, H-4^{AQ}), 7.32–7.30 (d, 1H, H-2^{AQ}), 4.02–4.00 (m, 1H, H-CH^a), 2.71 (s, 1H, NH), 1.39–1.37 (d, 6H, H-CH_3^b); FT-IR (KBr plate, ν cm^{-1}): 3243.42 (m, ν_{N-H}), 1627.72 (m, δ_{N-H}), 1662.25 (vs, br, $\nu_{C=O}$).

2.4.2 Data of 4-AQ

Red powder; mp = 81–82°C; Yield, 93%; $R_f = 0.65$; ^{1}H NMR (TMS, δ ppm): 8.31–8.29 (q, 1H, H-6^{AQ}), 8.22–8.20 (q, 1H, H-7^{AQ}), 7.92–7.82 (m, 2H, H-5^{AQ}, H-8^{AQ}), 7.67–7.64 (t, 1H, H-3^{AQ}), 7.54–7.53 (d, 1H, H-4^{AQ}), 7.29–7.27 (d, 1H, H-2^{AQ}), 3.48–3.43 (q, 2H, H-CH_2^a), 2.80 (s, 1H, NH), 1.82–1.75 (m, 2H, H-CH_2^b), 1.61–1.52 (m, 2H, H-CH_2^c), 1.04–1.01 (t, 3H, H-CH_3^d); FT-IR (KBr plate, ν cm^{-1}): 3245.67 (m, ν_{N-H}), 1630.83 (m, δ_{N-H}), 1662.59 (vs, br, $\nu_{C=O}$).

2.4.3 Data of 6^{c}-AQ

Red powder; mp = 182–183°C; Yield, 95%; $R_f = 0.67$; ^{1}H NMR (TMS, δ ppm): 8.32–8.30 (q, 1H, H-6^{AQ}), 8.22–8.20 (q, 1H, H-7^{AQ}), 7.92–7.82 (m, 2H, H-5^{AQ}, H-8^{AQ}), 7.65–7.61 (q, 1H, H-3^{AQ}), 7.53–7.51 (q, 1H, H-4^{AQ}), 7.34–7.31 (d, 1H, H-2^{AQ}), 3.76–3.72 (m, 1H, H-CH^{a}), 2.79 (s, 1H, NH), 1.86–1.51 (d, 8H, H-CH$_2^{b-c}$), 0.98–0.95 (m, 2H, H-CH$_2^{c}$); FT-IR (KBr plate, ν cm^{-1}): 3247.73 (m, ν_{N-H}), 1630.06 (m, δ_{N-H}), 1662.28 (vs, br, $\nu_{C=O}$).

2.4.4 Data of 6-AQ

Red powder; mp = 80–81°C; Yield, 91%; $R_f = 0.65$; ^{1}H NMR (TMS, δ ppm): 8.28–8.26 (q, 1H, H-6^{AQ}), 8.20–8.18 (q, 1H, H-7^{AQ}), 7.90–7.80 (m, 2H, H-5^{AQ}, H-8^{AQ}), 7.64–7.60 (q, 1H, H-3^{AQ}), 7.51–7.49 (q, 1H, H-4^{AQ}), 7.24–7.13 (d, 1H, H-2^{AQ}), 2.80 (s, 1H, NH), 1.82–1.75 (m, 2H, H-CH$_2^{b}$), 1.55–1.50 (m, 2H, H-CH$_2^{c}$), 1.43–1.36 (m, 4H, H-CH$_2^{d-e}$), 0.95–0.92 (t, 3H, H-CH$_3^{f}$); ^{13}C NMR (400 MHz, CD_3COCD_3, r.t., TMS, δ ppm): 184.46 (C═O), 182.91 (C═O), 151.85, 135.32, 134.94, 134.52, 134.02, 133.06, 132.96, 126.48, 126.23, 118.07, 114.87, 112.53 (C of benzene rings), 42.56 (NH—*C*H$_2$), 31.39–13.40 (11*C*$^{b-f}$); FT-IR (KBr plate, ν cm^{-1}): 3242.77 (m, ν_{N-H}), 1627.57 (m, δ_{N-H}), 1665.81 (vs, br, $\nu_{C=O}$).

2.4.5 Data of 10-AQ

Red powder; mp = 82–83°C; Yield, 87%; $R_f = 0.63$; ^{1}H NMR (TMS, δ ppm): 8.33–8.30 (q, 1H, H-6^{AQ}), 8.23–8.20 (q, 1H, H-7^{AQ}), 7.94–7.82 (m, 2H, H-5^{AQ}, H-8^{AQ}), 7.70–7.64 (t, 1H, H-3^{AQ}), 7.55–7.52 (q, 1H, H-4^{AQ}), 7.30–7.28 (d, 1H, H-2^{AQ}), 3.50–3.43 (q, 2H, H-CH$_2^{a}$), 2.84 (s, 1H, NH), 1.86–1.76 (m, 2H, H-CH$_2^{b}$), 1.60–1.50 (m, 2H, H-CH$_2^{c}$), 1.46–1.30 (m, 12H, H-CH$_2^{d-i}$), 0.91–0.86 (t, 3H, H-CH$_3^{j}$); FT-IR (KBr plate, ν cm^{-1}): 3296.63 (m, ν_{N-H}), 1628.73 (m, δ_{N-H}), 1661.70 (vs, br, $\nu_{C=O}$).

2.4.6 Data of 12-AQ

Orange powder; mp = 83.8–84.1°C; Yield, 84%; $R_f = 0.75$; ^{1}H NMR (TMS, δ ppm): 8.29–8.27 (q, 1H, H-6^{AQ}), 8.21–8.18 (q, 1H, H-7^{AQ}), 7.90–7.81 (m, 2H, H-5^{AQ}, H-8^{AQ}), 7.65–7.61 (q, 1H, H-3^{AQ}), 7.52–7.50 (q, 1H, H-4^{AQ}), 7.25–7.23 (d, 1H, H-2^{AQ}), 3.45–3.40 (q, 2H, H-CH$_2^{a}$), 2.80 (s, 1H, NH), 1.83–1.76 (m, 2H, H-CH$_2^{b}$), 1.56–1.50 (m, 2H, H-CH$_2^{c}$), 1.45–1.29 (m, 16H, H-CH$_2^{d-k}$), 0.90 (t, 3H, H-CH$_3^{l}$); ^{13}C NMR (400 MHz, CD_3COCD_3, r.t., TMS, δ ppm): 184.47 (C═O), 182.91 (C═O), 151.87, 135.33, 134.94, 134.53, 134.03, 133.07, 132.96, 126.48, 126.24, 118.09, 114.88, 112.54 (C of benzene rings), 42.54 (NH-*C*H$_2$), 31.74–13.44 (11*C*$^{b-l}$); FT-IR (KBr plate, ν cm^{-1}): 3296.44 (m, ν_{N-H}), 1629.03 (m, δ_{N-H}), 1661.94 (vs, br, $\nu_{C=O}$).

2.4.7 Data of 14-AQ

Orange powder; mp = 89–90°C; Yield, 90%; $R_f = 0.75$; ^{1}H NMR (TMS, δ ppm): 8.32–8.30 (q, 1H, H-6^{AQ}), 8.22–8.20 (q, 1H, H-7^{AQ}), 7.92–7.82 (m, 2H, H-5^{AQ}, H-8^{AQ}), 7.68–7.64 (q, 1H, H-3^{AQ}), 7.55–7.53 (q, 1H, H-4^{AQ}), 7.30–7.27 (d, 1H, H-2^{AQ}), 3.47–3.44 (q, 2H, H-CH$_2^{a}$), 2.80 (s, 1H, NH), 1.83–1.80 (m, 2H, H-CH$_2^{b}$), 1.58–1.51 (m, 2H, H-CH$_2^{c}$), 1.46–1.29 (m, 20H, H-CH$_2^{d-m}$), 0.90–0.87 (t, 3H, H-CH$_3^{n}$); FT-IR (KBr plate, ν cm^{-1}): 3298.17 (m, ν_{N-H}), 1628.94 (m, δ_{N-H}), 1661.54 (vs, br, $\nu_{C=O}$).

2.4.8 Data of 16-AQ

Orange powder; mp = 89–90°C; Yield, 82%; $R_f = 0.75$; ^{1}H NMR (TMS, δ ppm): 8.32–8.30 (d, 1H, H-6^{AQ}), 8.22–8.20 (d, 1H, H-7^{AQ}), 7.90–7.80 (m, 2H, H-5^{AQ}, H-8^{AQ}), 7.66–7.62 (t, 1H, H-3^{AQ}), 7.55–7.53 (d, 1H, H-4^{AQ}), 7.28–7.25 (d, 1H, H-2^{AQ}), 3.48–3.43 (q, 2H, H-CH$_2^{a}$), 2.61 (s, 1H, NH), 1.85–1.78 (m, 2H, H-CH$_2^{b}$), 1.60–1.53 (m, 2H, H-CH$_2^{c}$), 1.47–1.31 (m, 24H, H-CH$_2^{d-o}$), 0.90–0.88 (t, 3H, H-CH$_3^{p}$); FT-IR (KBr plate, ν cm^{-1}): 3241.88 (m, ν_{N-H}), 1628.44 (m, δ_{N-H}), 1669.11 (vs, br, $\nu_{C=O}$).

2.4.9 Data of 18-AQ

Orange powder; mp = 85–86°C; Yield, 87%; $R_f = 0.76$; ^{1}H NMR (TMS, δ ppm): 8.23 (d, 1H, H-6^{AQ}), 8.21–8.20 (d, 1H, H-7^{AQ}), 7.94–7.82 (m, 2H, H-5^{AQ}, H-8^{AQ}), 7.70–7.67 (t, 1H, H-3^{AQ}), 7.56–7.53 (q, 1H, H-4^{AQ}), 7.31–7.28 (q, 1H, H-2^{AQ}), 3.50–3.43 (q, 2H, H-CH$_2^{a}$), 2.85 (s, 1H, NH), 1.87–1.76 (m, 2H, H-CH$_2^{b}$), 1.56–1.51 (m, 2H, H-CH$_2^{c}$), 1.45–1.29 (m, 28H, H-CH$_2^{d-q}$), 0.91–0.86 (t, 3H, H-CH$_3^{r}$); FT-IR (KBr plate, ν cm^{-1}): 3242.34 (m, ν_{N-H}), 1628.74 (m, δ_{N-H}), 1669.36 (vs, br, $\nu_{C=O}$).

2.5 Preparation of vesicles

Two equimolar solutions, one of *n*-AQ and the other of CD, were prepared with triply distilled water and methanol (1:1, by volume). All sample solutions for the investigation were freshly prepared by diluting the stock solution. Considering the poor solubility of *n*-AQ, the proper concentration for the vesicular formation was tested and chosen to be 10^{-5} mol/l, for both *n*-AQ and CD. The sample solutions contained the same volume of *n*-AQ (2×10^{-5} mol/l) and of CD (2×10^{-5} mol/l) solutions, and then ultrasonicated for 20 min at 300 K before detection.

The effect of an external stimulus was investigated by adding an external irritant to the sample solutions.

2.6 Detection of the stoichiometries of the n-AQ/β-CD complex

Two equimolar stock solutions (10^{-4} mol/l), one of *n*-AQ (*g*) and the other of β-CD (*h*), were prepared. A set of

working solutions was obtained by mixing V_g ml of the *n*-AQ compound stock solution with $(V_t - V_h)$ ml of the stock β-CD solution, where V_t is a fixed total volume and V_g is a variable value (from 0 to 10 ml, $0 \leq V_g \leq V_t$).

2.7 Measure of the fluorescence spectrum of 18-AQ in the presence of different concentrations of β-CD

A set of working solutions was obtained by mixing different amounts of the β-CD stock solution with the 18-AQ compound stock solution of 10^{-5} mol/l. Nos 0–5 represent the β-CD concentrations of 0, 10^{-5}, 2×10^{-5}, 3×10^{-5}, 4×10^{-5} and 5×10^{-5} mol/l, respectively.

2.8 Atomic-based MD simulation

In order to construct the intersimulation model, a bilayer that contained nine pairs of 10-AQ/β-CD units was placed in the middle of a tetragonal box of $42 \times 42 \times 70$ Å^3, surrounded by a mixture consisting of water and methanol (molar ratio = 2.25:1; Figure 7). The system yields approximately 10^{-5} molar solutions according to the experimental data. Application of periodic boundary conditions with a unit cell produces a vesicle bilayer perpendicular to the *z*-axis.

The system was first minimised 10,000 steps of steepest descent minimisation to avoid bad contacts. Then, the MD simulation was carried out in the NVT ensemble with constant particle number, volume and temperature of 298 K with a time step of 1 fs. The non-bonded interactions were cut off at 12 Å, and long-range electrostatic interactions were accounted for using the Ewald method. The COMPASS force field was employed in the simulation. The molecular modelling software, Materials Studio 4.3 from Accelrys, Inc., USA (http://accelrys.com/) was used to perform the calculations.

2.9 Stains of living cells

In a separate culture flask, 10 ml of MCF-7 cells with a density of 10^5 ml^{-1} were cultured in a wall-adhesive mode. Twenty microlitres of the vesicle solution of 12-AQ/β-CD (10^{-5} mol/l) were added to the liquid medium in a culture flask and mixed well. The cells were then successively cultured in a cell incubator for 3 h. The basic culture medium was then removed and washed three times with 5 ml of PBS. In the same way, REW-264.7 cells were cultured and then 18-AQ/β-CD (10^{-5} mol/l) and 18-AQ (10^{-5} mol/l) were used to stain both cell lines.

3. Results and discussion

Multiple factors, including the tail length (ranging from C_0 to C_{18}), the composition of the solvent (methanol: water = 1:0, 2:1, 1:1, 1:2, 0:1, by volume) and the host molecules (β-CD or HP-β-CD), affected the aggregates formed by the 'supramolecular amphiphiles'. Self-assembled aggregates such as vesicles (Figure 2), nanospheres (Figure 3) and micelles were formed, as can be seen from the TEM images. It can be inferred that methanol is adverse to the formation of vesicles, as listed in the Supporting Information, available online. This may be attributed to the single hydrogen-binding site and to an extent to methanol occupying the cavity of CD (*1*, *9–11*). It is known that due to the solvophobic theory, the composition of solvents may affect the microstructure in solution (*22*). It was thought that vesicles formed in the solvent of pure water might have promising applications in biomaterials. However, these vesicles were not stable, because of the extremely low solubility of *n*-AQ in an aqueous solution. Although CDs play a role in increasing the solubility of the guest molecules, precipitation appeared when undisturbed for 2 h, which suggests that the pure-water system is more unstable. Therefore, the addition of the organic solvent is necessary. From the TEM observation, it was also found that the regularity of the aggregates in water/methanol = 1:1 (by volume) is much better, which could pave the way for the theoretical research of supramolecular amphiphiles, such as the critical tail length to form vesicles. HP-β-CD is more soluble in an aqueous solution than β-CD; however, the existence of hydroxypropyl is also a hindrance to the inclusion of β-CD and guest molecules (*23*).

3.1 Morphologies and sizes of the vesicles

Closed vesicular structures (Figure 2) were observed clearly by TEM with phosphotungstic acid as the staining agent, which is a reliable and versatile method for studying the microaggregates. The spheres with core–shell structures were observed. These observations are similar to the vesicular morphologies obtained by Zhang et al. (*12*, *13*). The particles show a significant contrast between the centre and the periphery, which is the typical character of the vesicular structure (*24*, *25*). For further confirmation of the effect of the inclusion complexes, the individual solutions of *n*-AQs or CDs were detected by TEM separately and no regular aggregates were found. DLS measurements were also performed to measure the average diameters of vesicles, and the results for the six systems are shown in Figure 4. As an example, Figure 2(a) shows that the particles are spherical with diameters ranging from 190 to 210 nm, which is slightly smaller than the results found by DLS. This seems reasonable because TEM and DLS showed solid and swollen vesicles, respectively (*24*, *25*). Furthermore, typical particle aggregates formed by 14-AQ/β-CD and 18-AQ/HP-β-CD in pure water are shown in Figure 3.

SEM (Figure 5) and EFM (Figure 6) were also undertaken to investigate the vesicular structure. SEM imaging provided further evidence for the formation of vesicular structures. The technology of sputter-coating with gold on

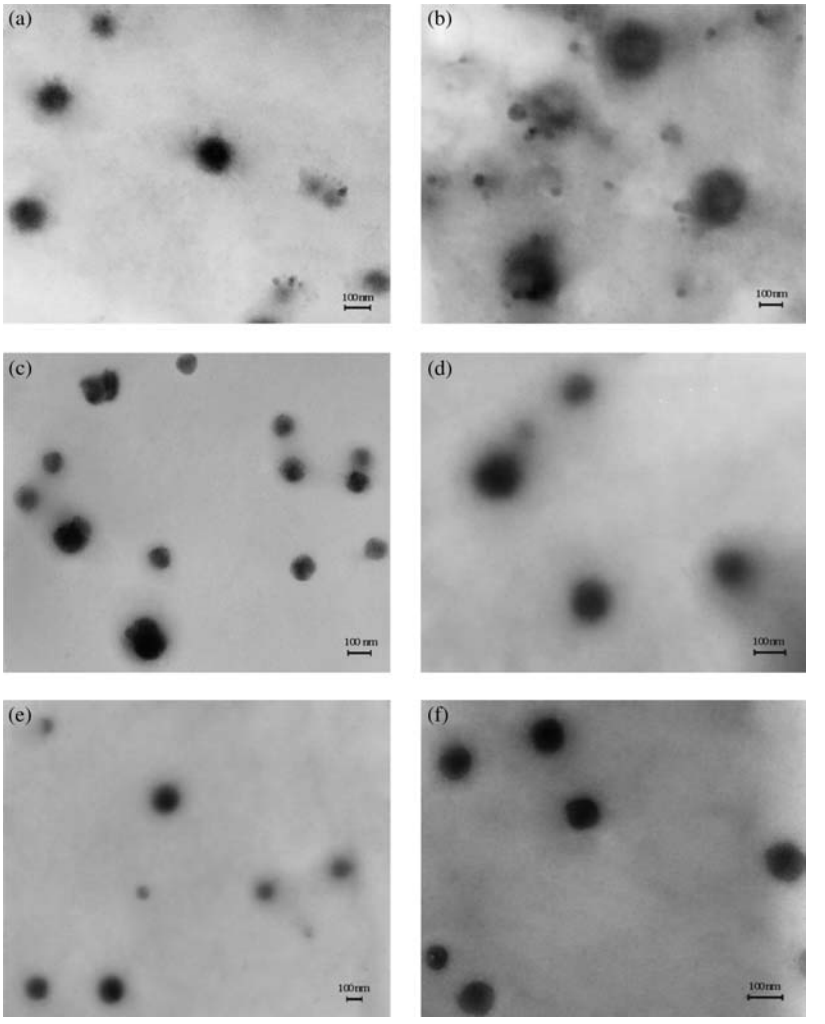

Figure 2. TEM images of (a) 6-AQ/β-CD; (b) 10-AQ/β-CD; (c) 12-AQ/β-CD; (d) 14-AQ/β-CD; (e) 16-AQ/β-CD; (f) 18-AQ/β-CD in a solution of water/methanol = 1:1 (by volume) with phosphotungstic acid as the negative staining agent; scale bars = 100 nm.

the microaggregates' surface can be applied to prepare organic samples for SEM (*26–28*). However, the solid vesicular structure may collapse to form holes for the high-energy impacts as observed in SEM (*29*, *30*), which also suggested the sensitive property of the vesicles. The colour contrast of the SEM images, hollow caves with diameters ranging approximately from 100 to 200 nm, was close to the results of TEM and DLS.

Anthraquinone (AQ) and its derivatives can be applied as probes in biochemistry (*31–33*), analytical

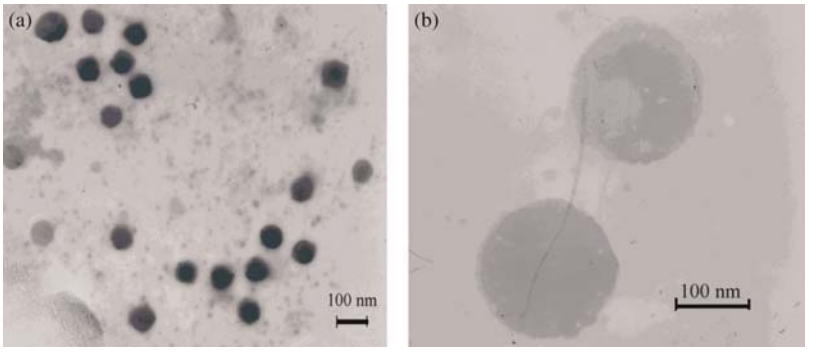

Figure 3. TEM images of (a) 14-AQ/β-CD; (b) 18-AQ/HP-β-CD in pure water; scale bars = 100 nm.

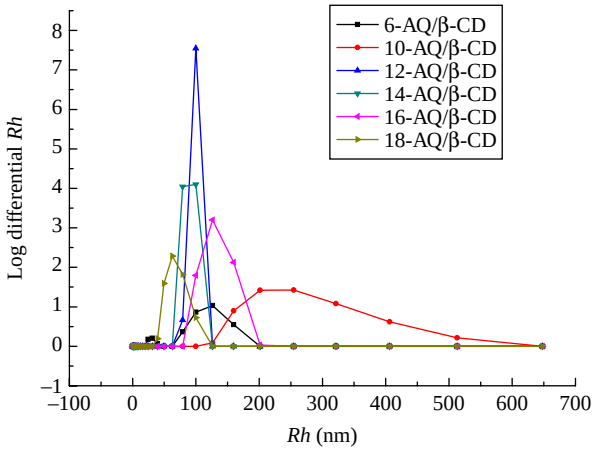

Figure 4. DLS of *n*-AQ/β-CD in a solution of water/methanol = 1:1 (by volume) at r.t.

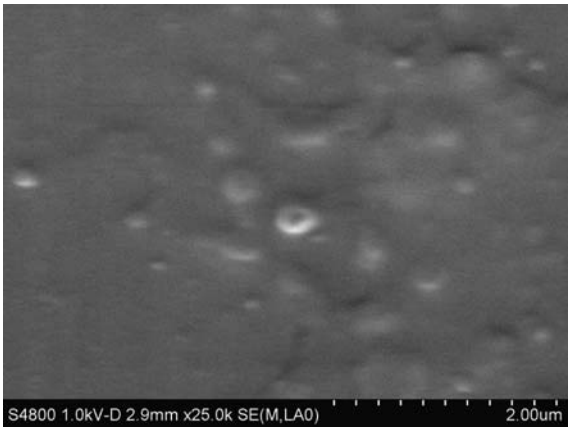

Figure 5. SEM images of 18-AQ/β-CD at r.t.; scale bar = 2 μm.

chemistry (*34*) and physical chemistry (*35*, *36*) because of their strong fluorescence. 12-AQ/β-CD and 18-AQ/β-CD in a solution of water/methanol = 1:1 (by volume) were taken as examples. Under the fluorescence microscope, several drops of *n*-AQ/β-CD solution placed on the glass slide revealed clear microspheres with strong fluorescence and were found to be in typical Brownian movement (Figure 6(a)). The study on the Brownian movement of nanoparticles is useful in the analysis of the vesicle-gel transformation process (*37*). The bilayers could not be clearly recognised because of the limited amplification of EFM (× 100) (*38*, *39*). However, it is clear that sphere structures were formed and dispersed homogeneously in the solution. The property of fluorescence was successfully implanted into the vesicles.

3.2 *The possible formation mechanism of the vesicles*

The complex stoichiometry was confirmed by UV spectroscopy using Job's plot method. 18-AQ/β-CD and 6-AQ/β-CD were chosen as the examples. The experimental curve (Figure 7) describes the interactions between *n*-AQ and β-CD in the solution of water/methanol (1:1, by volume). It reached its maximum at a molar fraction of 0.5, which indicates that the complex stoichiometry of 18-AQ/β-CD and 6-AQ/β-CD in a solution of water:methanol (1:1, by volume) is 1:1 (*40*, *41*).

It was found that the fluorescence intensity of 18-AQ was strengthened when β-CD was added into the solution (Figure 8). According to the literature (*42*), these small but significant changes in the absorption intensity upon addition of β-CD to 18-AQ suggested the formation of an 18-AQ/β-CD complex in the solution of water/methanol (1:1, by volume). The fluorescence enhancement was attributed to the β-CD cavity, which can supply a microenvironment and to a large extent protect the guest AQ from contacting the surrounding water molecules. This led to an increase in the fluorescence quantum yield and intensity, which suggested that 18-AQ entered the cavity of β-CD to form supramolecular inclusion (*43*).

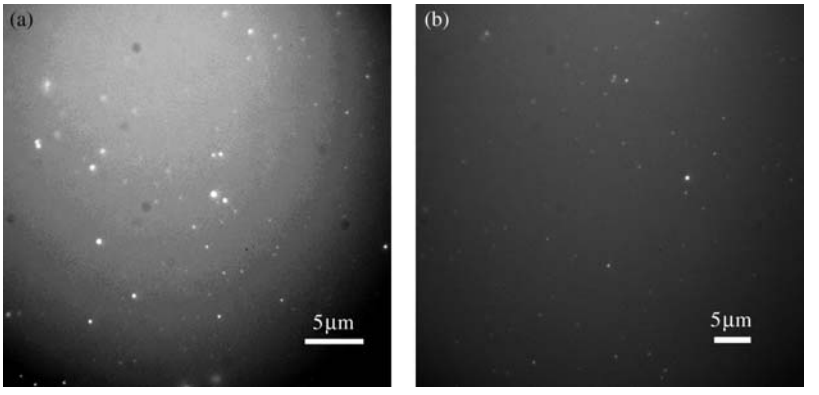

Figure 6. EFM images of *n*-AQ/β-CD in a solution of water/methanol = 1:1 (by volume) at r.t. excited at 340 nm with mercury lamp: (a) × 60, 18-AQ/β-CD; (b) × 60, 6-AQ/β-CD; scale bars = 5 μm.

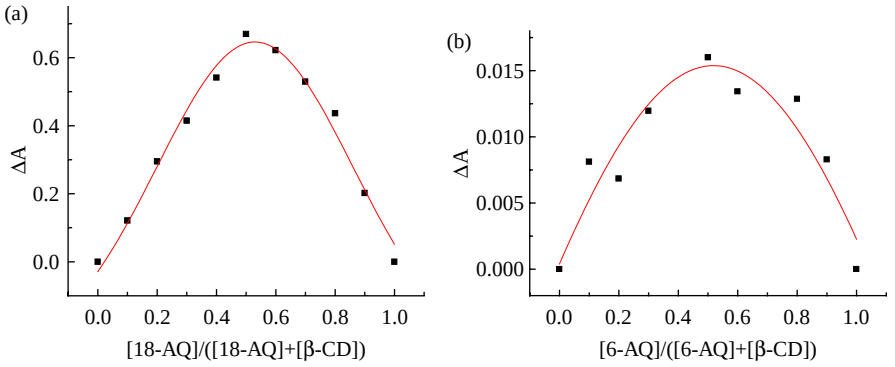

Figure 7. Job's curve of the inclusion complex of (a) 18-AQ/β-CD, the Δ*A* in the wavelength of 266 nm was picked to obtain Job's curve; (b) 6-AQ/β-CD in the solvent (*V*(methanol):*V*(water) = 1:1) by UV, the Δ*A* in the wavelength of 516 nm was picked to obtain Job's curve.

The most direct and dependable evidence for the supramolecular inclusion of 18-AQ and β-CD is from ^{1}H NMR, which is one of the most powerful tools for realising supramolecular assemblies in solution. The concentration of 18-AQ/β-CD was so low that the peak of 18-AQ was almost undistinguishable from the baseline. However, clear shifts of β-CD were observed, which demonstrated the inclusion phenomenon (*44–46*).

In the presence of 18-AQ, almost all the hydrogen resonances of β-CD showed chemical shifts (Table 2). 18-AQ is a relatively large molecule compared with other regular guest molecules, such as benzene, ferrocene and adamantane, so 18-AQ may exert a broad effect to hydrogen atoms H1–H6 of β-CD.

CDs, which are cyclic oligosaccharides with hydrophobic cavities, have the capability to bind substrates selectively to form inclusion complexes (*1–5*). The primary criterion for the inclusion of a guest molecule within the host's cavity is its size and then other factors such as strict fit, van der Waals' interactions, hydrogen bond and so on. A possible inclusion of *n*-AQ into β-CD, with a cavity opening size of 6.5 Å, would be an axial inclusion, due to a suitable size of the guest molecules in this direction (*47–49*). However, the inclusion of *n*-AQ/β-CD is supposed to be only partial (*50–52*). In this case, the unsubstituted benzene ring was inside the host's cavity while the central ring bearing two C═O groups as well as the alkyl-substituted aminobenzene ring remained outside the cavity, and participated in H-bonding with the secondary hydroxyl groups of β-CD (*51*, *52*) (Scheme 1). The proposed structures for inclusion complexes of β-CD with *n*-AQ are given in Scheme 1. Based on the discussion above, the anthraquinone group of *N*-alkylamino-L-anthraquinone would partly enter the cavity of β-CD to construct the hydrophilic 'head', and the alkyl chain outside the cavity would perform the role of the hydrophobic 'tail' to form a peculiar type of 'amphiphilic surfactant'. Furthermore, the inclusion phenomenon was investigated by UV and fluorescence spectra. Based on the experimental results, a possible mechanism was proposed, as illustrated in Scheme 1. While being ultrasonicated and well dispersed in the solution, the supramolecular complex could self-assemble into vesicles. The above analysis indicates that the inclusion phenomenon was the main control of the vesicle formation.

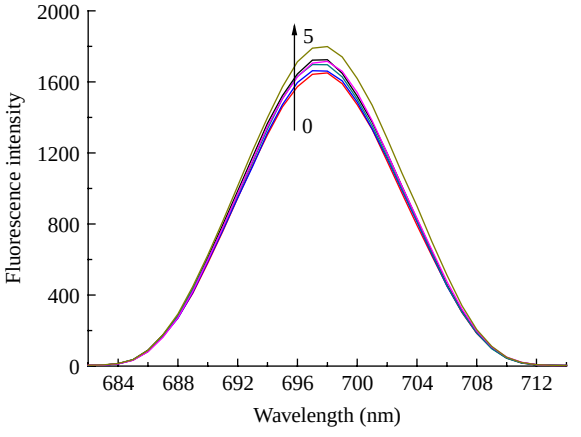

Figure 8. Fluorescence intensity spectra of 18-AQ and β-CD in the solution of water/methanol (1:1, by volume), Nos 0–5 represent the solution with β-CD concentrations of 0, 10^{-5}, 2×10^{-5}, 3×10^{-5}, 4×10^{-5}, 5×10^{-5} and 6×10^{-5} mol/l, respectively. The excitation wavelength is 380 nm.

3.3 *Demonstration of the vesicle model*

An MD simulation was performed to validate the possibility of the above mechanism model. Atomic-based MD simulations can play a powerful role in indicating the properties at a microscopic level and are considered as complements to experiments. In this paper, a classical MD simulation of the 10-AQ/β-CD vesicle structure was performed to investigate the possibility of the above-mentioned mechanism model. Since it could be very time-consuming to obtain a spontaneous bilayer structure from a random initial configuration, we started the simulations from the pre-assembled state, as has been reported in most other

Table 2. The chemical shifts of ^{1}H NMR from H-1 to H-6.

Entry	H-1	H-2	H-3	H-4	H-5	H-6
δ (β-CD)[a]	4.977	3.696	3.585	3.499	3.859	3.800
δ (18-AQ/β-CD)[b]	–	3.746	3.593	3.511	3.913	3.853
$\Delta\delta$	–	0.050	0.008	0.012	0.054	0.053

[a] All the samples were measured in a solution of D_2O and CD_3OD (1:1, by volume), $T = 300$ K.
[b] The complex of 18-AQ/β-CD was measured with a concentration of 10^{-5} mol/l in order to coincide with the concentration of the vesicle formation.

simulation systems (*53–59*). Although the bilayer takes a relatively long time to form, once formed, it is stable as shown in Figure 9. Employing the space-extension principle, the part of the bilayer shown in Figure 9 can be generalised to the whole vesicle. The obtained results were similar to the suggested mechanism shown in Scheme 1, which further confirmed our presumption. This was the first time that MD simulation experiments were used to study the mechanism of vesicles self-assembled by 'supramolecular amphiphiles'.

This is also the first time to study the effect of the 'tail' length to the formation of vesicles based on 'supramolecular amphiphiles'. 6-AQ, 10-AQ, 12-AQ, 14-AQ, 16-AQ and 18-AQ were able to self-assemble into vesicles with β-CDs, while 6^c-AQ, 4-AQ, 3^i-AQ, *N*-methylamino-L-AQ, L-aminoanthraquinone and AQ were not able to self-assemble. The inability to self assemble is likely because the hydrophobic tail chains are too short and decrease the 'hydrophobic–hydrophobic interaction' between the building blocks. From the above results, the hydrophobic 'tail' of the alkyl chain with six carbon atoms was considered as the lower limit to self-assemble into vesicular structures in this supramolecular system. Moreover, the fact that 6-AQ and 6^c-AQ show different results in this system should be emphasised: the length but not the volume of the hydrophobic 'tail' seems to play a more important role in the formation of vesicles' bilayers.

3.4 *The properties of the vesicles*

3.4.1 *Sensitive and multi-responsive properties of the vesicles*

The vesicles disappeared upon the addition of equimolar $CuCl_2$. The shift of the UV peaks of *n*-AQ in the presence of Cu^{2+} indicates that *n*-AQ can complex with this ion (Figure 10). From the literature (*60*, *61*), it is known that Cu^{2+} easily binds to the N atom. The vesicles also

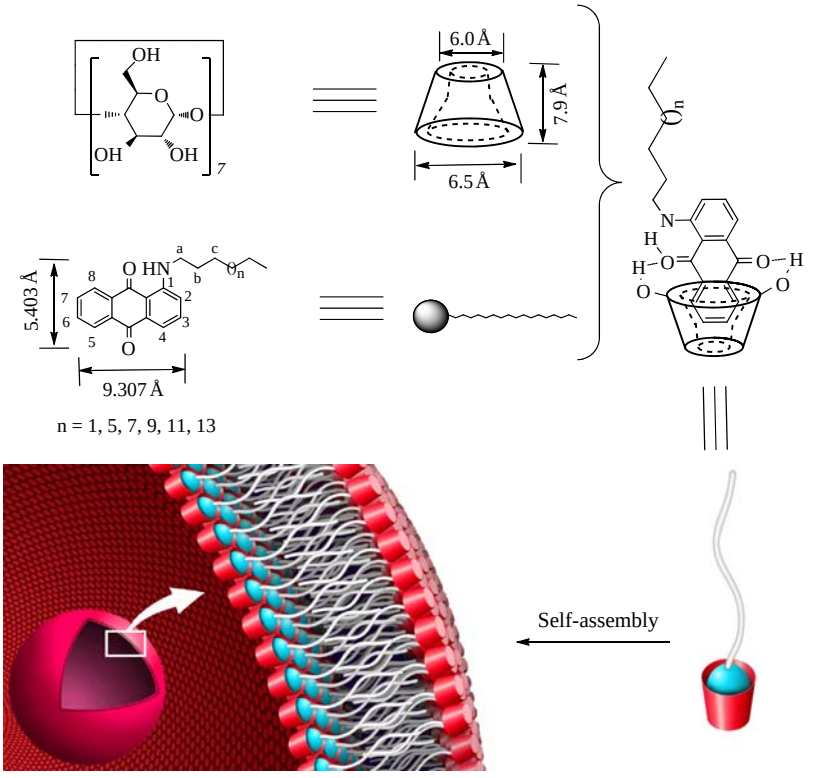

Scheme 1. The possible mechanism of the vesicle formation based on the experimental results.

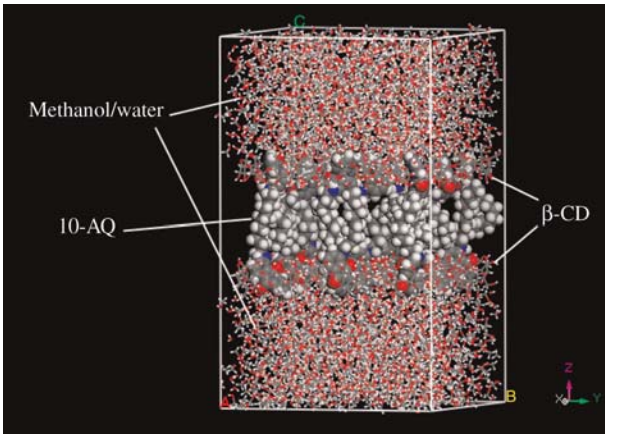

Figure 9. Results of the MD simulation of 10-AQ/β-CD in the solution of methanol/water = 1:1 by volume.

responded to H^+. The UV spectrum, similar to the results of the addition of $CuCl_2$, also had a significant variation with the addition of acetic acid, which indicates the change from secondary amine to quaternary ammonium.

Meanwhile, the UV adsorption related to 18-AQ/Cu^{2+} and 18-AQ/H^+ changed in the presence of β-CD, which suggests that β-CD can still include 18-AQ upon addition of Cu^{2+} or H^+ (*62*). However, both Cu^{2+} and H^+ are harmful to the formation of vesicles from the TEM observations. This may be attributed to the increase in the electrostatic repulsive force between the 'building blocks', which makes it difficult for the aggregates to form (Scheme 3). The results described may provide new opportunities in mimicking some biological processes or building new pH-controlled drug-release system and pH-responsive materials, especially for the drug release at cancer cells, which can cause an acidic environment (*63–66*).

Ampicillin, piroxicam, simvastatin and amoxicillin (Scheme 2, the concentrations were all chosen as 10^{-5} mol/l) were separately added into the vesicle solution of 18-AQ/β-CD to investigate its response to the drug molecules. As indicated in TEM, vesicles were destroyed with the addition of the three drugs, which may be due to the inclusion competition between *n*-AQ and the drug molecule (Scheme 3), since it was reported that these drugs could form 1:1 inclusion with β-CD (*67*). Those non-covalent interactions of receptors and ligands, or the host and the guest at the vesicle surfaces resemble the recognition processes at biological membranes. This property may further our understanding in biological membranes through the biomimetic supramolecular chemistry of vesicles (*68–71*).

3.5 *Application of the vesicle system in cell staining*

Vesicles, enclosing a volume with membranes consisting of a bilayer or a multilayer of specific molecules, have drawn increasing attention for the hope of applications in drug and gene delivery (*72–77*), nanoreactors (*78*, *79*) and artificial cell membranes (*69–71*). However, vesicles, to a certain extent, seem to have more potential than practical application.

From the above experimental results, it is clear that the vesicles are multi-responsive, or in other words, the vesicles are sensitive. Hence, we can deduce that when introduced into the cell suspension with a complicated composition, vesicles may collapse, and the guest

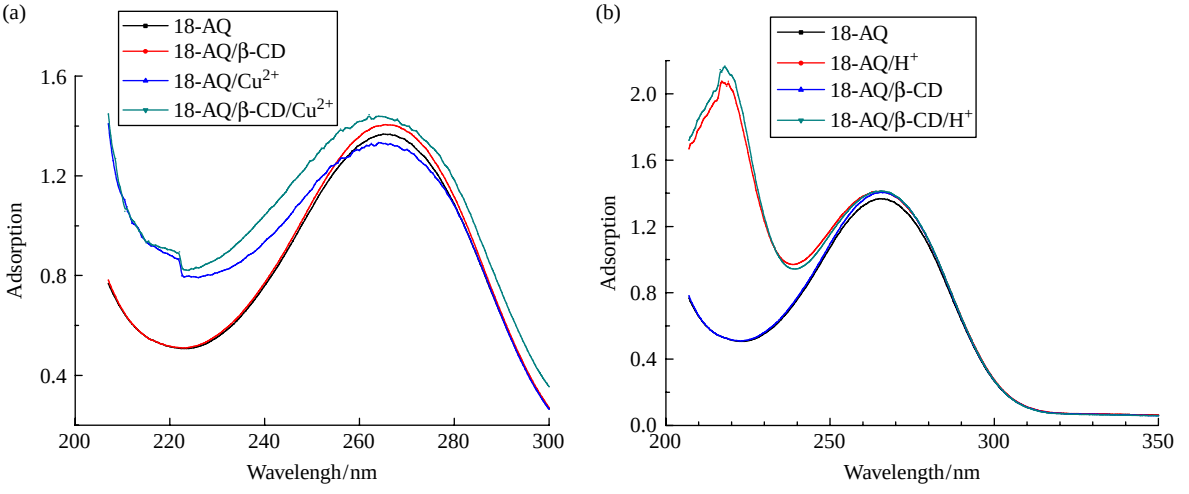

Figure 10. (a) UV spectra of 18-AQ (black line), 18-AQ/β-CD (red line), the mixture of 18-AQ and $CuCl_2$ (blue line, solution of [$CuCl_2$] = 10^{-5} mol/l was as the baseline), the mixture of 18-AQ/β-CD and $CuCl_2$ (green line, the solution of [$CuCl_2$] = 10^{-5} mol/l was as the baseline). [18-AQ] = [18-AQ/β-CD] = [$CuCl_2$] = 10^{-5} mol/l. T = 300 K; (b) UV spectra of 18-AQ (black line), the mixture of 18-AQ and acetic acid (red line), 18-AQ/β-CD (blue line), the mixture of 18-AQ/β-CD and acetic acid (green line). [18-AQ] = [18-AQ/β-CD] = [acetic acid] = 10^{-5} mol/l. T = 300 K.

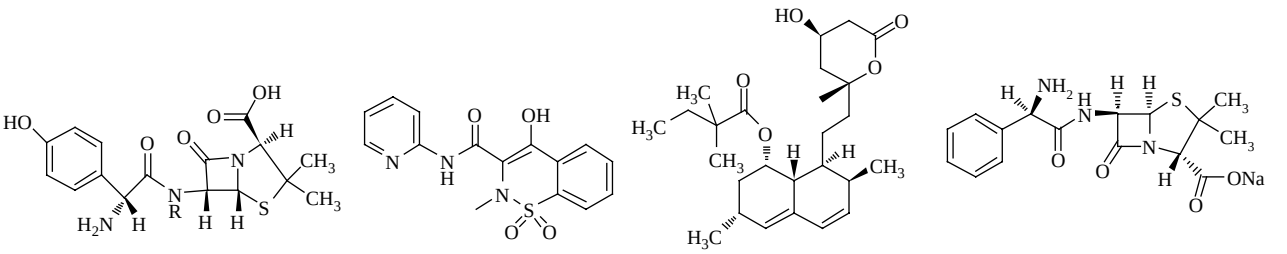

Scheme 2. The chemical structures of the selected external guests.

molecules may be released to stain the cells. Images of cells with blue fluorescence were taken using UV ray-excitation mode. The cells were distinct when viewed with the fluorescence microscope (Figure 11(b) and (d)). Images of cells by fluorescence microscopy were in good accordance with the images under natural lighting. Since cells which are not fluorescently stained cannot be observed by microscope under fluorescence conditions, we could judge that *n*-AQ was adsorbed in the cell membrane through the collapse of vesicles. Control experiments showed that 18-AQ (10^{-5} mol/l) in methanol/water (1:1, solution by volume) could only stain the cells with very weak but corresponding fluorescence, which can further demonstrate the important role played by the vesicles. Another control experiment showed that by staining the cells with Rhodamine B (also 10^{-5} mol/l in methanol/water (1:1, solution by volume)) also offers a weaker and more vague fluorescence (Figure 12).

The images showed that the cells could be stained evenly and with strong luminous intensity. The samples were observed by fluorescence microscopy for more than 3 h and the fluorescent intensity did not decrease, which offers a longer fluorescence lifetime and better homogeneity compared with other cell stainers, such as Rhodamine B (Figure 12). Although methanol is adverse to most cells, a trace addition (20 μl into 10 ml) can be overlooked.

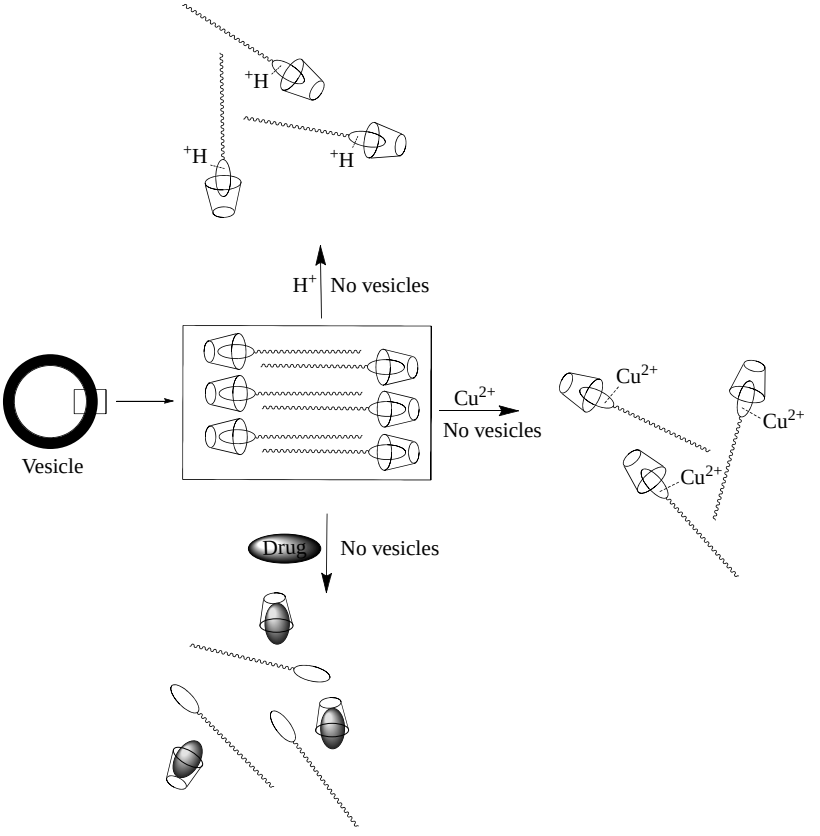

Scheme 3. Multi-responsive vesicles.

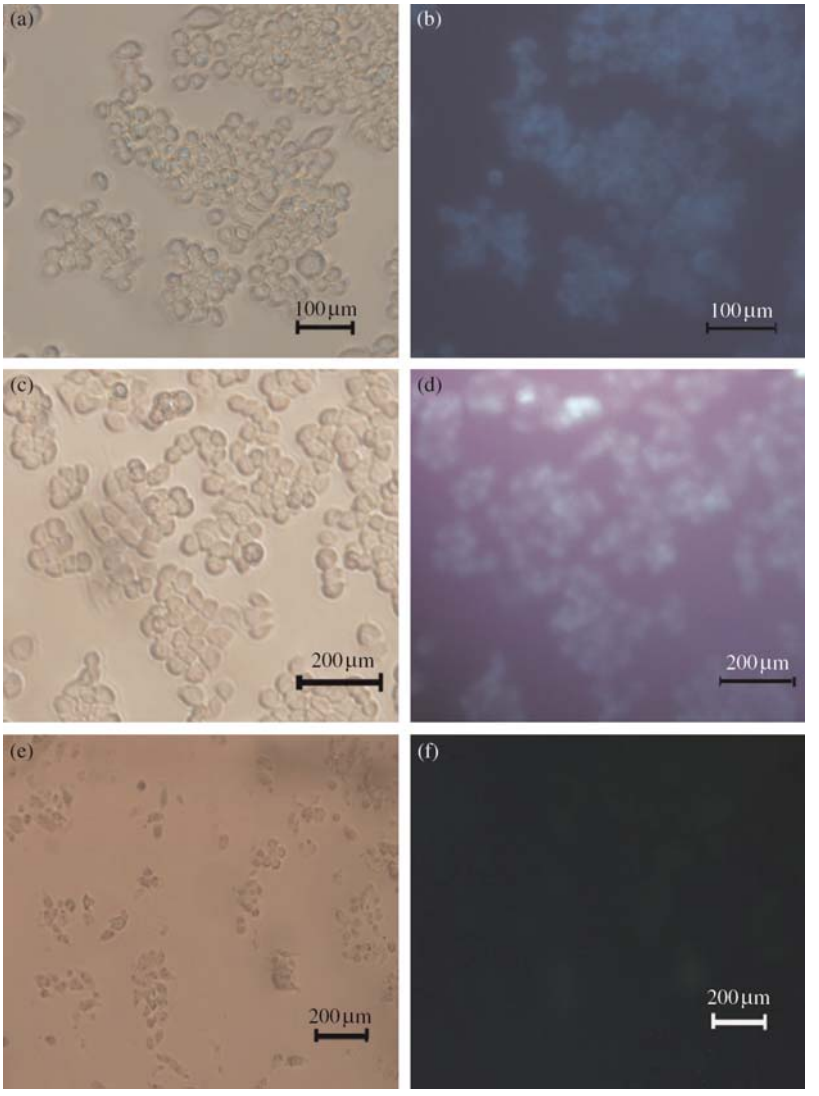

Figure 11. Microscopy images of living cells after treating with the vesicular solution: REW264.7 cells stained with vesicles of 18-AQ/β-CD: (a) under natural lighting; (b) in fluorescence microscopy; RM-1 cells stained with vesicles of 12-AQ/β-CD (c) under natural light; (d) in fluorescence microscopy; REW264.7 cells stained with 18-AQ (10^{-5} mol/l in methanol/water = 1:1 solution by volume): (e) under natural lighting and (f) in fluorescence microscopy.

Our methods may provide a new approach to detect cellular localisation. This may also lead to a new way to achieve targeted release of some anti-cancer drugs via the replacement of guest molecules, especially when CDs, which have molecule recognition property, are the guest molecules. Furthermore, we did not observe any sign of morphological damage to the cells after the treatment, demonstrating the low toxicity of the system of *n*-AQ/β-CD (*80*).

The collapse of vesicles may be due to the change of the environment, especially the change of the solution from methanol/water to an aqueous solution. For then, vesicles collapse and *n*-AQ is released from the CD cavity and adsorbed by the cell membrane, since *n*-AQ's solubility is very low in an aqueous solution. The non-covalent bond between CDs and glycoprotein or other molecules in the cell membrane also plays an important role in the progress of AQ adsorption. The instability and sensitivity of supramolecular vesicles formed by 'amphiphilic surfactant' were successfully applied here. In summary, through a 'recognition–release–fusion' process, the dyes with fluorescence capacity can be attached to the cell membrane. The study on the effect of fluorescent vesicles on the inner cell organelles is still in progress.

4. Conclusion

In summary, we report the designation, preparation and application of a novel fluorescent vesicle system. The strategy was demonstrated as follows: in order to achieve

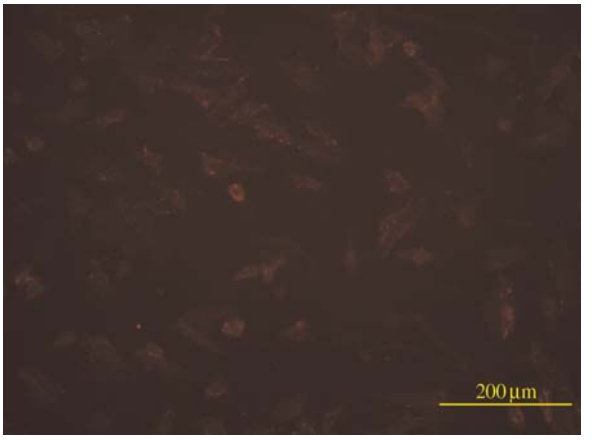

Figure 12. Fluorescence microscopy images of human aortic smooth muscle cells after treating with Rhodamine B.

the goal, nine *n*-AQs with different lengths of alkyl were synthesised by the direct reaction of L-nitroanthraquinone and alkylamines to act as the guest molecules. With the inclusion of *n*-AQ and β-CD, the supramolecular complex can self-assemble into vesicular structures in the methanol/water solvent, which were visualised by TEM, SEM, DLS and EFM. The property of fluorescence was successfully implanted into vesicles, which was observed by EFM. The possible mechanism of the vesicle formation was suggested based on the results of UV, fluorescence spectrum and MD simulation. The vesicles were sensitive and multi-responsive to external stimuli. Furthermore, the vesicles were successfully applied in the staining of living cells and the possible staining approach was also suggested. We believe that the supramolecular vesicles will serve useful in the fields of biomaterials, cell-mimic, design of intelligent materials and molecule machines.

Acknowledgements

This work was supported by the NSFC (Grant No. 20625307), National Basic Research Program of China (973 Program, 2009CB930103) and Graduate Independent Innovation Foundation of Shandong University (GIIFSDU). We thank Ms Carla R. Christ from Santa Barbara, USA and Dr Z. Yang from Université Pierre et Marie Curie: Paris 6 for editing the manuscript for English corrections.

References

(1) Szejtli, J. *Chem. Rev.* **1998**, *98*, 1743–1753.
(2) Sortino, S.; Mazzaglia, A.; Scolaro, L.M.; Merlo, F.M.; Valveri, V.; Sciortino, M.T. *Biomaterials* **2006**, *27*, 4256–4265.
(3) Falvey, P.; Lim, C.W.; Darcy, R.; Revermann, T.; Karst, U.; Giesbers, M.; Marcelis, A.T.M.; Lazar, A.; Coleman, A.; Reinhoudt, D.; Ravoo, B.J. *Chem. Eur. J.* **2005**, *11*, 1171–1180.
(4) Mazzaglia, A.; Ravoo, B.J.; Gambadauro, R.D.P.; Mallamace, F. *Langmuir* **2002**, *18*, 1945–1948.
(5) Wang, J.; Jiang, M. *J. Am. Chem. Soc.* **2006**, *128*, 3703–3708.
(6) Bugler, J.; Sommerdijk, N.A.J.M.; Visser, A.J.W.G.; Hoek, A.; Nolte, R.J.M.; Engbersen, J.F.J.; Reinhoudt, D.N. *J. Am. Chem. Soc.* **1999**, *121*, 28–33.
(7) Ravoo, B.J.; Darcy, R. *Angew. Chem., Int. Ed.* **2000**, *39*, 4324–4326.
(8) Sallas, F.; Darcy, R. *Eur. J. Org. Chem.* **2008**, *6*, 957–969.
(9) Connors, K.A. *Chem. Rev.* **1997**, *97*, 1325–1357.
(10) Rekharsky, M.V.; Inoue, Y. *Chem. Rev.* **1998**, *98*, 1875–1917.
(11) Douhal, A. *Chem. Rev.* **2004**, *104*, 1955–1976.
(12) Zhang, H.; Shen, J.; Liu, Z.; Bai, Y.; An, W.; Hao, A. *Carbohydr. Res.* **2009**, *344*, 2028–2035.
(13) Zhang, H.; An, W.; Liu, Z.; Hao, A.; Hao, J.; Shen, J.; Zhao, X.; Sun, H.; Sun, L. *Carbohydr. Res.* **2009**, *345*, 87–96.
(14) Jing, B.; Chen, X.; Wang, X.; Yang, C.; Xie, Y.; Qiu, H. *Chem. Eur. J.* **2007**, *13*, 9137–9142.
(15) Guo, M.; Jiang, M.; Zhang, G. *Langmuir* **2008**, *24*, 10583–10586.
(16) Abdel-Rahem, R.; Hoffmann, H. *J. Colloid Interface Sci.* **2007**, *312*, 146–155.
(17) Joshi, J.V.; Aswal, V.K.; Goyal, P.S. *Phys. B* **2007**, *391*, 65–71.
(18) Yuet, P.K.; Blankschtein, D. *Langmuir* **1996**, *12*, 3819–3827.
(19) Zhai, L.; Zhao, M.; Sun, D.; Hao, J.; Zhang, L. *J. Phys. Chem. B* **2005**, *109*, 5627–5630.
(20) Israelachvili, J.N. *Intermolecular and Surface Forces*; Academic Press: New York, 1994.
(21) Reubke, K. US patent 1976, 4076736.
(22) Ray, A. *Nature* **1971**, *231*, 313–315.
(23) Sun, T.; Hao, A.; Shen, J.; Song, L. *Synth. Commun.* **2009**, *39*, 4309–4314.
(24) Wang, L.; Liu, H.; Hao, J. *Chem. Commun.* **2009**, 1353–1355.
(25) He, Y.; Fu, P.; Shen, X.; Gao, H. *Micron* **2008**, *39*, 495–516.
(26) Mazzaglia, A.; Angelini, N.; Lombardo, D.; Micali, N.; Patane, S.; Villari, V.; Scolaro, L.M. *J. Phys. Chem. B* **2005**, *109*, 7258–7265.
(27) Qian, J.; Wu, F. *Macromolecules* **2008**, *41*, 8921–8926.
(28) Yang, J.; Keller, M.W.; Moore, J.S.; White, S.R.; Sottos, N.R. *Macromolecules* **2008**, *41*, 9650–9655.
(29) Kamilya, T.; Pal, P.; Mahato, M.; Talapatra, G.B. *Mat. Sci. Eng. C-Bio. Sci.* **2009**, *29*, 1480–1485.
(30) Yuan, P.; Yang, S.; Wang, H.; Yu, M.; Zhou, X.; Lu, G.; Zou, J.; Yu, C. *Langmuir* **2008**, *24*, 5038–5043.
(31) Kumamoto, S.; Watanabe, M.; Kawakami, N.; Nakamura, M.; Yamana, K. *Bioconj. Chem.* **2008**, *19*, 65–69.
(32) Qiao, C.; Bi, S.; Sun, Y.; Song, D.; Zhang, H.; Zhou, W. *Spectrochim. Acta A* **2008**, *70*, 136–143.
(33) Liu, Y.; Hu, N. *Biosens. Bioelectron.* **2007**, *23*, 661–667.
(34) Yamaguchi, A.; Nakano, M.; Nochi, K.; Yamashita, T.; Morita, K.; Teramae, N. *Anal. Bioanal. Chem.* **2006**, *386*, 627–632.
(35) Zhu, L.; Khairutdinov, R.F.; Cape, J.L.; Hurst, J.K. *J. Am. Chem. Soc.* **2006**, *128*, 825–835.
(36) Bhattacharya, S.; Subramanian, M. *J. Chem. Soc., Perkin Trans.* **1996**, *2*, 2027–2034.
(37) Jesorka, A.; Markstrom, M.; Karlsson, M.; Orwar, O. *J. Phys. Chem. B* **2005**, *109* (31), 14759–14763.
(38) Xu, Y.; Wang, G.; Zhao, X.; Jiang, X.; Li, Z. *Langmuir* **2009**, *25*, 2684–2688.

(39) Horbaschek, K.; Hoffmann, H.; Thunig, C. *J. Colloid Interface Sci.* **1998**, *206*, 439–456.
(40) MacCarthy, P. *Anal. Chem.* **1978**, *50*, 2165.
(41) Guo, M.; Jiang, M.; Zhan, G. *Langmuir* **2008**, *24*, 10583–10586.
(42) Wu, Q.; Zhu, M.; Wei, S.; Song, K.; Liu, L.; Guo, Q. *J. Incl. Phenom. Macro.* **2005**, *52*, 93–100.
(43) Wang, Y.; Zhu, M.; Ding, X.; Ye, J.; Liu, L.; Guo, Q. *J. Phys. Chem. B* **2003**, *107*, 14087–14093.
(44) Schneider, H.J.; Hacket, F.; Rudiger, V. *Chem. Rev.* **1998**, *98*, 1755–1785.
(45) Demarco, P.V.; Thakkar, A.L. *Chem. Commun.* **1970**, 2–4.
(46) Redenti, E.; Szente, L.; Szejtli, J. *J. Pharm. Sci.* **2001**, *90*, 979–986.
(47) Jiang, H.; Sun, H.; Zhang, S.; Hua, R.; Xu, Y.; Jin, S.; Gong, H.; Li, L. *J. Incl. Phenom. Macro.* **2007**, *58*, 133–138.
(48) D'Anna, F.; Riela, S.; Gruttadauria, M.; Meo, P.L.; Noto, R. *Tetrahedron* **2005**, *61*, 4577–4583.
(49) D'Anna, F.; Riela, S.; Meo, P.L.; Noto, R. *Tetrahedron* **2004**, *60*, 5309–5314.
(50) Shamsipur, M.; Yari, A.; Sharghi, H. *Spectrochim. Acta A* **2005**, *62*, 372–376.
(51) Petrova, S.S.; Kruppa, A.I.; Leshina, T.V. *Chem. Phys. Lett.* **2005**, *407*, 260–265.
(52) Dang, X.; Nie, M.; Tong, J.; Li, H. *J. Electroanal. Chem.* **1998**, *448*, 61–67.
(53) Wang, Z.; Larson, R.G. *J. Phys. Chem. B* **2009**, *113*, 13697–13710.
(54) Maillet, J.B.; Lachet, V.; Coveney, P.V. *Phys. Chem., Chem. Phys.* **1999**, *1*, 5277–5290.
(55) Yakovlev, D.S.; Boek, E.S. *Langmuir* **2007**, *23*, 6588–6597.
(56) Piotrovskaya, E.M.; Vanin, A.A.; Smirnova, N.A. *Mol. Phys.* **2006**, *104*, 3645–3651.
(57) Boek, E.S.; den Otter, W.K.; Briels, W.J.; Iakovlev, D. *Philos. T.R. Soc. A* **2004**, *362*, 1625–1638.
(58) Padding, J.T.; Boek, E.S.; Briels, W.J. *J. Phys.: Condens. Matter* **2005**, *17*, 3347–3353.
(59) Briels, W.J.; Mulder, P.; den Otter, W.K. *J. Phys.: Condens. Matter* **2004**, *16*, 3965–3974.
(60) Masakatsu, S.; Motomu, K. *Chem. Rev.* **2008**, *108*, 2853–2873.
(61) Bernardo, K.; Leppard, S.; Robert, A.; Commenges, G.; Dahan, F.; Meunier, B. *Inorg. Chem.* **1996**, *35*, 387–396.
(62) Dermody, D.L.; Peez, R.F.; Bergbreiter, D.E.; Crooks, R.M. *Langmuir* **1999**, *15*, 885–890.
(63) Bhujwalla, Z.M.; McCoy, C.L.; Glickson, J.D.; Gillies, R.J.; Stubbs, M. *Br. J. Cancer* **1998**, *78*, 606–611.
(64) Beselli, R.; Renzi, G.; Morello, R.; Altieri, F. *J. Craniofac. Surg.* **2007**, *18*, 1051–1054.
(65) Yamagata, M.; Tannock, I.F. *Br. J. Cancer* **1996**, *73*, 1328–1334.
(66) Tannock, I.F.; Rotin, D. *Cancer* **1989**, *49*, 4373–4389.
(67) Aki, H.; Ikeda, H.; Yukawa, M. *J. Ther. Anal. Calorim.* **2009**, *95*, 421–426.
(68) Voskuhl, J.; Ravoo, B. *Chem. Soc. Rev.* **2009**, *38*, 495–505.
(69) Lehn, J.M. *Science* **2002**, *295*, 2400–2403.
(70) Shimizu, T.; Masuda, M.; Minamikawa, H. *Chem. Rev.* **2005**, *105*, 1401–1444.
(71) Discher, D.E.; Eisenberg, A. *Science* **2002**, *297*, 967–973.
(72) Allen, T.M.; Cullis, P.R. *Science* **2004**, *303*, 1818–1822.
(73) Korobko, A.V.; Backendorf, C.; van der Maarel, J.R.C. *J. Phys. Chem. B* **2006**, *110*, 14550–14556.
(74) Guo, X.; Szoka, F. *Acc. Chem. Res.* **2003**, *36*, 335–341.
(75) Hogset, A.; Prasmickaite, L.; Selbo, P.K.; Hellum, M.; Engesaeter, B.O.; Bonsted, A.; Berg, K. *Adv. Drug Deliv. Rev.* **2004**, *56*, 95–115.
(76) Zou, P.; Pan, C.Y. *Macromol. Rapid Commun.* **2008**, *29*, 763–771.
(77) Jan, J.S.; Lee, S.J.; Carr, C.S.; Shantz, D.F. *Chem. Mater.* **2005**, *17*, 4310–4317.
(78) Christensen, S.M.; Stamou, D. *Soft Matter* **2007**, *3*, 828–836.
(79) Sauer, M.; Haefele, T.; Graff, A.; Nardin, C.; Meier, W. *Chem. Commun.* **2001**, 2452–2453.
(80) Zhou, C.; Shen, H.; Guo, Y.; Xu, L.; Niu, J.; Zhang, Z.; Du, Z.; Chen, J.; Song, L. *J. Colloid Interface Sci.* **2010**, *344*, 279–285.